Proceedings of 12th Cambridge Workshop on Cool Stars, Stellar Systems, & The Sun, 2003 University of Colorado.

Emission Measure Distributions in Active Binary Systems

J. Sanz-Forcada

Harvard-Smithsonian Center for Astrophysics

Abstract.

Generally, the study of coronal structure in other cool stars different from the Sun is limited to 2–T or 3–T emission measure fits, and only a few cases are described with a continuous distribution of values in temperature. In this work it is presented the study of 22 active binary systems and 6 single stars, the widest sample of stars to date for which the emission measure distribution is described as a continuous distribution. The analysis covers the range log T(K)=4.0–7.4, making use of EUVE iron lines and IUE data to describe the behavior in the corona and transition region. Conclusions are derived from the quiescent and flaring stages in 6 active binary systems, and the whole sample includes a variety of spectral types in giant and dwarf stars. The calculated distributions do not match, totally or partially, those predicted by current models.

1. Introduction

The increase in spectral resolution achieved with the *Extreme Ultraviolet Explorer* (EUVE) respect to previous satellites, allowed for first time the development of a continuous Emission Measured Distribution (EMD) for many stars. The EMD is the best tool developed to identify the structure of stellar coronae. The Emission Measure basically tells how the emitting material is distributed with the emitting temperature, allowing to identify the energy balance in the transition region and corona of the star.

In this work a combination of IUE low resolution ($\sim$6 Å) spectra, covering $\lambda\lambda$ 1100–1950, and EUVE spectra covering the range $\lambda\lambda$ 70–750 with the short, mid and long-wavelength (SW, MW and LW) spectrographs ($\lambda/\Delta\lambda$ $\sim$200–400), is used to obtain the EMD in a wide sample of stars. A sample of 22 active binary systems have been chosen for this porpose, as well as 6 single stars or wide binaries, used for comparison (Sanz-Forcada, Brickhouse,&Dupree, 2001a; Sanz-Forcada, Brickhouse, & Dupree, 2001b,c). First non-solar EMD analyses revealed a very different EMD configuration to that observed in the Sun for active stars like Capella, 44 Boo or V711 Tau (see Dupree et al., 1993; Brickhouse & Dupree, 1998; Griffiths & Jordan, 1998, and references therein).

Although some of the stars in the sample have been already analyzed by different authors, the addition of *all* the observations available in the EUVE archive for each of the objects by June 2001, greatly improves the statistics for these targets, allowing the identification of weaker lines useful to better the temperature coverage in the EUVE region (log T[K]$\sim$5.7–7.4).

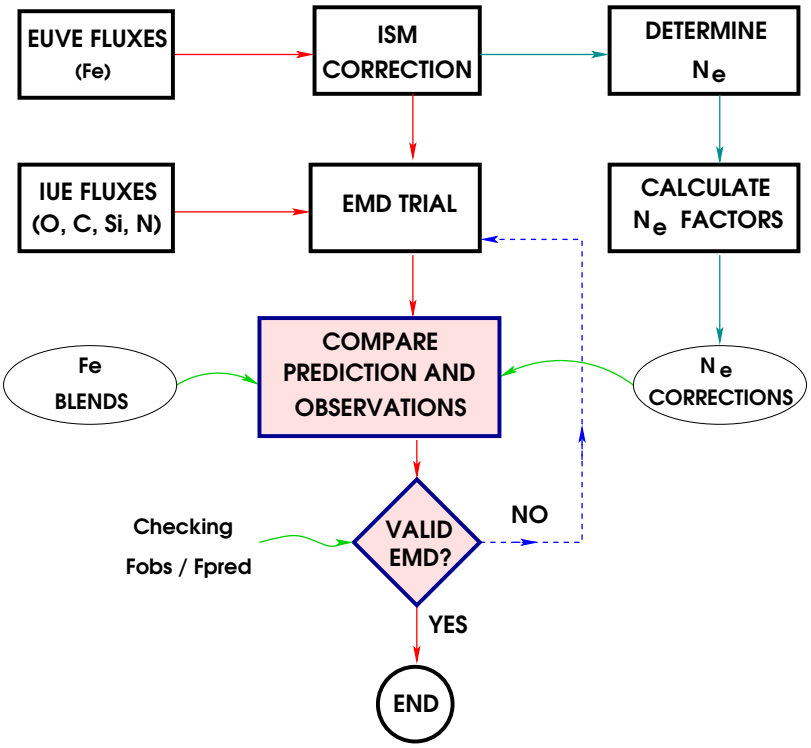

Figure 1. Technique employed in the determination of the Emission Measure Distribution (EMD).

The method employed in this work makes use of a line-based analysis, considering the whole emissivity function of every spectral line, instead of the habitual use of only the value at the peak of the emissivity. The employment of the whole function allow to tighten better the EMD at each point. The atomic models used are those by Raymond (1988) for non-iron lines, based on solar photospheric abundances by Allen (1973), and Brickhouse, Raymond, & Smith (1995) for iron lines, modified to account for iron abundance by Anders & Grevesse (1989). The technique is outlined in Fig. 1, and follow the next steps: measurement of the line fluxes in IUE and EUVE (only iron lines are used in the latter, while carbon lines dominate the EMD in the IUE range); EUVE lines need to be corrected by the effects of the interestellar medium absorption, and then an initial EMD is proposed. This EMD is used in the main program to predict theoretical line fluxes with the emissivities given by the atomic models, and the resulting fluxes are then compared with those measured in the spectra. The inspection of the discrepancies observed will help in the modification of successive EMDs to be tried in an iterative process, until the fluxes best match. Two important corrections are introduced in the main program: first the inclusion of blends by iron lines to calculate theoretical line fluxes in the EUV, and

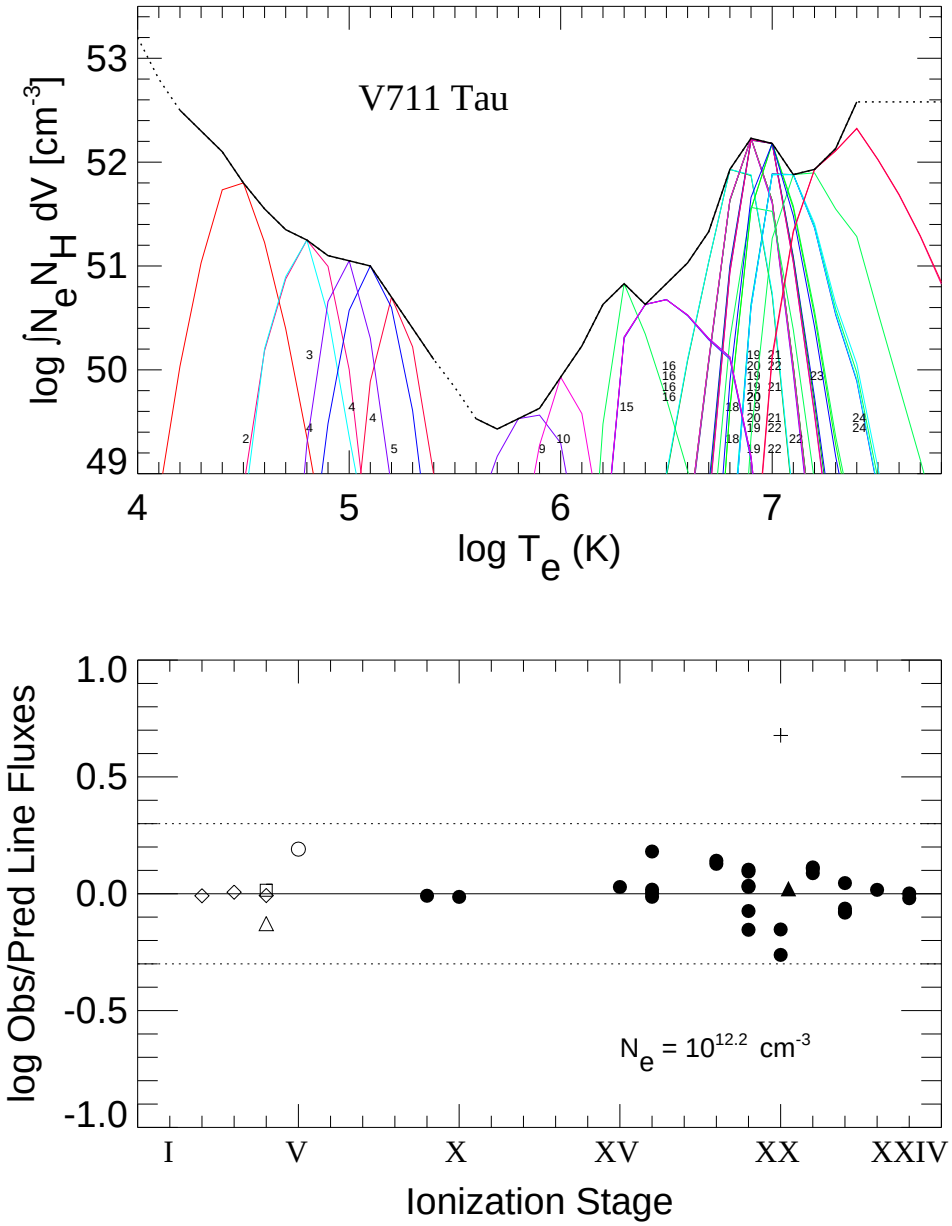

Figure 2. *Upper*: EMD for the EUVE summed spectrum combined with an IUE quiescent spectrum for V711 Tau. Thin lines represent the relative contribution function for each ion (the emissivity function multiplied by the EMD at each point). *Lower*: Observed to predicted line ratios for the ion stages in top figure. The dotted lines denote a foactor of 2. Symbols used are open circles for N, diamonds for C, squares for O, open triangles for Si, filled circles for Fe ions with S/N greater than 4, inverted filled triangles for Fe ions with S/N between 3 and 4, and crusses for lines with S/N lower than 3.

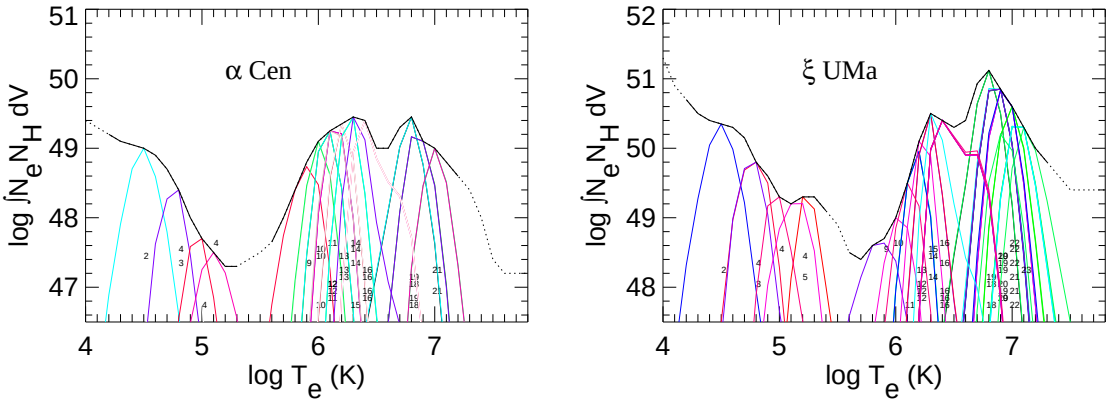

Figure 3. EMD obtained for α Cen AB and ξ UMa

second the use of different sets of emissivities depending on the electron density employed. The latter is calculated from line flux ratios of iron lines[1].

A good example is given by the system V711 Tau (HR 1099, see Fig. 2). The addition of up to 1 Ms of observations allows to identify lines formed in the whole range covered by EUVE. The modification of the value of the emission measure at any temperature affects the ratio between predicted and observed fluxes of several lines, allowing the obtention of a well constrained EMD.

2. Emission Measure Distribution

The analysis of the whole sample (28 stars) reveals a dominance of stars with a conspicous narrow enhancement or "bump" around log T(K)$\sim$6.9, but some of the objects selected allow to see some "evolution" in the shape of the EMD from the less active stars (α Cen AB, Procyon) to the most active (V711 Tau, UX Ari, II Peg) stars. α Cen AB (G2V+K1V) is expected to be dominated by the B component, with a 2:1 flux rate in the ROSAT/HRI band (Schmitt, 1998) but with a non-neglictible contribution from the A component. The EMD of α Cen (Fig. 3) recalls quite closely that from the Sun in quiescent conditions until log T(K)$\sim$6.5, where the solar EMD continues a downslope. But the best solution found for α Cen displays a peak around log T(K)$\sim$6.8, although in this case the peak is not very well constrained since the number of lines is small. Similar peak is found for Procyon, that reaches the same general levels in the EMD if it is considered the size of the stars[2].

An intermediate case towards the very active stars would be represented by ξ UMa (Fig. 3), a system formed by two spectroscopic binaries (G0V/[M] + G5V/[K]), according to Griffin (1998). Lines observed in the UV band with

[1]Eventually some blends affecting these lines are re-evaluated when a better knowledge of the EMD is available.

[2]Since the emitting regions are distributed over the stellar surface, it is expected to find some dependency in the general level of the emission measure with the square of the stellar radius.

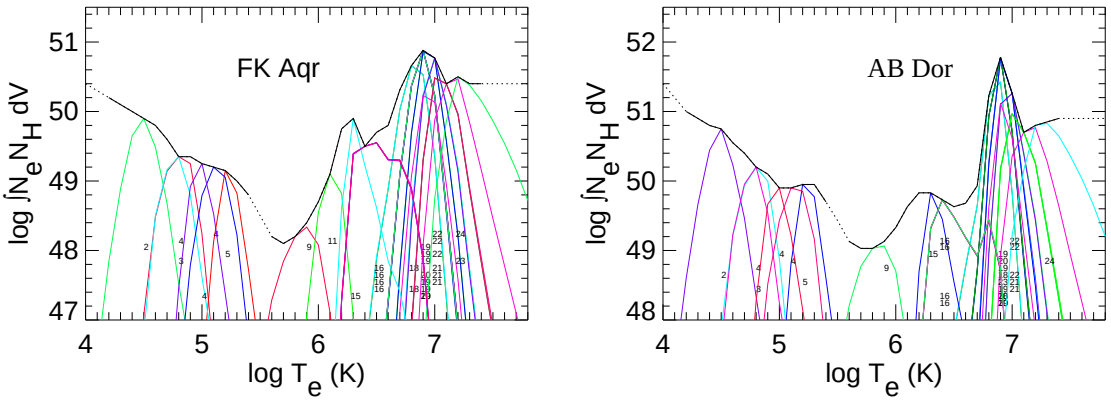

Figure 4. EMD obtained for FK Aqr and AB Dor

IUE show a dominance by the B component with a rate of 2:1, and hence it is assumed that most of the EUV emission will arise from the B component (Sanz-Forcada, 2001). This system begins to show a clear bimodality, with a dominant component peaking at log T(K)∼6.8, although with a decreasing amount of material at hotter temperatures. It is significant the presence of a well constrained second peak around log T(K)∼6.3, very similar to the shape of in the EMD for the active Sun.

Some of the stars in the sample begin to develop an increasingly important contribution of material with log T(K)$\gtrsim$7.1, as it is the case of FK Aqr (dM2/dM3), where the bump at log T(K)∼6.9 dominates the EMD, and there is a not so well constrained presence of a second bump peaking at log T(K)∼6.3 (Fig. 4).

The next step in activity is given by stars like V711 Tau (G5 IV/K1 IV, Fig. 2), where the EM goes on increasing at the highest temperatures marked by lines observable with EUVE. The presence of the bump log T(K)∼6.9 is very solid for most cases, and does not seem to follow any dependency on spectral type, luminosity class or even rotational period. Mass trasnfer in close binaries seems not to be the cause either, since objects like AB Dor or β Cet (Figs. 4,8) show a similar bump. Most of the objects where the EMD is dominated by this feature, have a high rotation rate (although cases like β Cet have the same bump dominating even for an *apparent* low rotation rate of v sin i∼4 km/s).

3. Effects of Flares in the EMD

The achievement of good statistics for some stars has allowed the separated analysis of flaring and quiescent stages. This kind of analysis were carried out for 6 stars: λ And (Sanz-Forcada et al., 2001a), V711 Tau, σ Gem, UX Ari and II Peg (Sanz-Forcada et al., 2001b), and AR Lac (Sanz-Forcada et al., 2001c). Fig. 5 displays the light curves corresponding to three flares in the systems λ And and σ Gem, showing a much longer duration and higher flux rates than the typical solar flares, indicating that this kind of flares do not

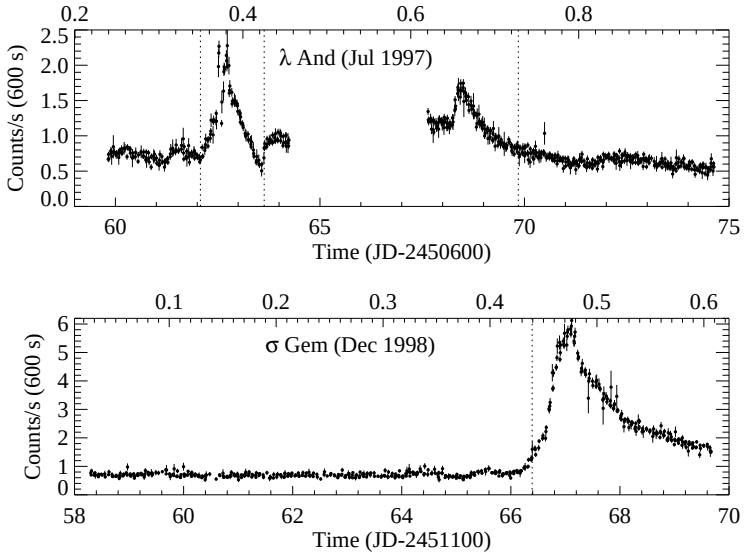

Figure 5. EUVE/DS light curves (600 s binning) as a function of Julian Date (lower axis) and orbtal phase (upper axis). At orbital phase 1.0 the primary star is located behind the secondary star (according to Table 1). Error bars mark a 1-σ level of error in the count rate. Only points with S/N higher than 5 are plotted. Vertical lines mark the separation between quiescent and flaring stages.

necessarily have the same effects in the EMD than solar-like flares. The spectral changes suffered by σ Gem during the large flare in 1998 are compared to the quiescent observations from the rest of the EUVE campaigns combined (Fig 6). The continuum experiments an increase similar to that found in the lines of Fe XXIII and Fe XXIV, those formed at highest temperatures observed with EUVE, indicating a major influence of the bremmstrahlung in this continuum, although many weak lines formed in the SW spectrum could also be enhanced by the flare.

Electron density measurements carried out from line ratios in the Fe XIX–XXII indicate high electron densities in the material formed around log T(K)$\sim$7.0, with values of log $N_e(cm^{-3}) \gtrsim 12.0$ for all the stars in the sample where measurements were available (all except Procyon), although for some of the objects the statistics are low, or there is only one density diagnostic available. A tendency has been also observed towards a higher electron density during flares in some of the stars, like λ And (Fig. 8).

The EMD estimated from the EUVE and IUE combined observations[3] is not well constrained in the region of the minimum EM, around log T(K)$\sim$5.8, but the general behavior in the EUV region points towards an increase in the whole EMD in the range log T(K)$\sim$6.0–7.4 (Fig. 7), with a slight increase in the slope below the bump at log T(K)$\sim$6.9 (see Sanz-Forcada et al., 2001b, for further details). In the cases of II Peg and V711 Tau it was possible to use IUE

[3]Note that IUE spectra are not simultaneous to those employed in the EUVE region, and some caution must be used prior to stablish a comparison.

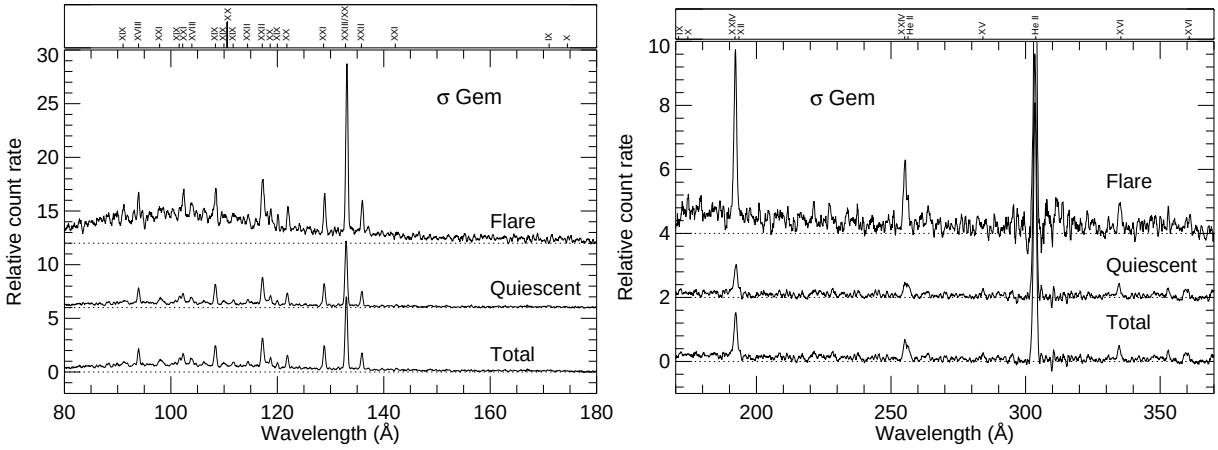

Figure 6. EUVE SW and MW spectra for σ Gem during flare and quiescent intervals, and the summed spectra. Ion stages of iron are marked in the top panel. Spectra are smoothed by 5 pixels. Dotted lines indicate the zero flux level of each spectrum.

spectra at the peak of a flare, showing an outstanding increase in the region around log T(K)$\sim$4.9 respect to the quiescent EMD.

4. Discussion

The active binary systems show a clearly different behavior to that observed in stars like the Sun, α Cen or Procyon. The case of V711 Tau shows the best statistics among the cases with emission in the range log T(K)$\sim$6.0–7.4, also supported by a good determination of the interstellar medium (ISM) absorption[4]. The EMD show 4 main features, also similar in other systems: (a) a decreasing slope (dEM/dT) in the low temperature range (log T[K]$\lesssim$5.6), that is mainly determined by C lines; (b) the minimum of the EMD, around log T(K)$\sim$5.7, similar to that previously found by Dupree et al. (1993) in Capella near log T(K)$\sim$5.8; (c) an increasing EMD from the minimum up to the maximum temperature observable; and (d), a narrow "bump" around log T(K)$\sim$6.9.

The presence of different abundances in the transition region and corona respect to those used by atomic models, can have some influence in the shape of the section (a) of the EMD, and in the determination of the position of the minimum (b) (specially dependent on the different metallicity of C and Fe). The general slope (c) observed underlying the bump (d) is 1.5 for the case of V711 Tau, corresponding to the slope predicted by conduction in coronal loops (see for instance, Jordan, 1996), although can reach higher values in other stars, with some dependence also on the determination of the ISM absorption[5]. But the

[4]A ratio of He I:H I=0.09 is used, with a value of $N_H(cm^{-2})=1.0\times10^{18}$ based on the Fe XVI λ335/λ361 lines flux ratio.

[5]Note that Fe XVI lines at 335 and 361 Åare used to partly constrain the EMD in the range log T(K)$\sim$6.3–6.8, and these lines are more affected by the value of the ISM used.

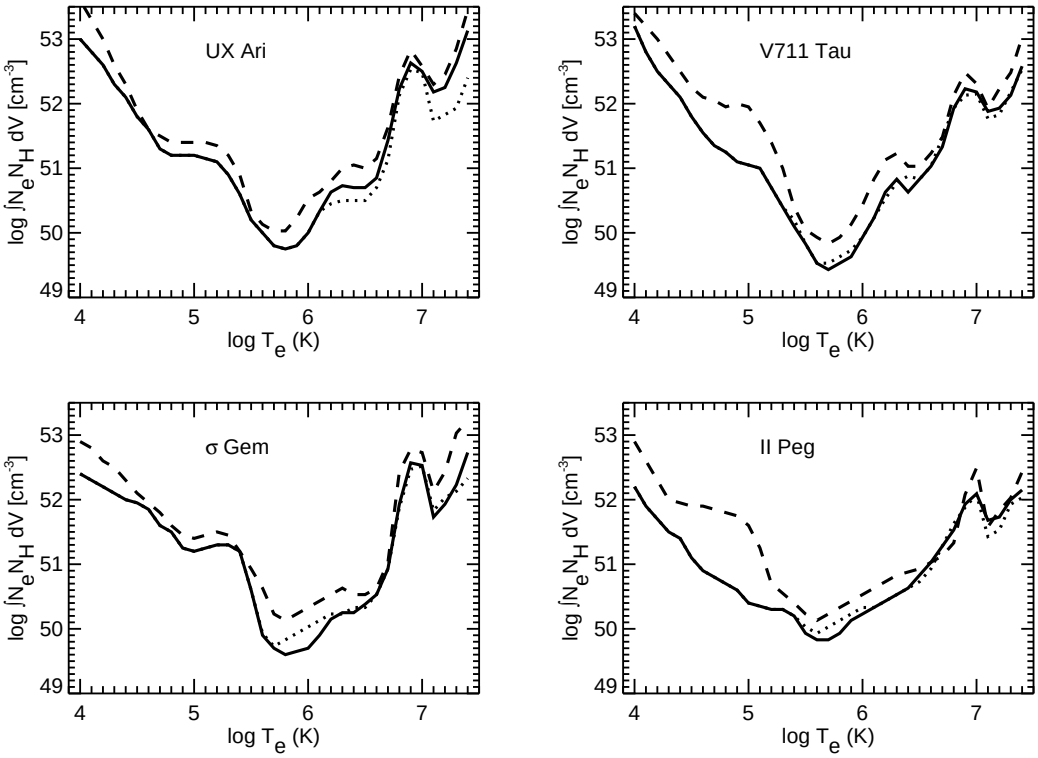

Figure 7. EMD of UX Ari, V711 Tau, σ Gem and II Peg during summed (solid line), flaring (dashed line) and quiescent (dotted line) stages.

possible first bump peaking around log T(K)$\sim$6.3, and in special the conspicous bump at log T(K)$\sim$6.9, can not be explained with simple hydrostatic loops with fixed cross-section, and need from additional effects, like expanding cross-sections in the loops (Schrijver, Lemen, & Mewe, 1989; Griffiths, 1999), or mass movements (Hussain, 2001). Another effect observed, the high electron densities measured from up to 5 iron lines fluxes ratios, with values of log N$_e(cm^{-3}) \gtrsim$12.0 at log T(K)$\sim$7.0 are not considered by current loop models. The only situation observed in the Sun where such high electron densities are observed in the corona, is during flares.

In the view of the models developed to date, the most likely explanation to the observed EMD in the region log T(K)$\sim$6.0–7.4 is the presence of two dominating kinds of loops. The first kind would be solar-like loops, and they peak around log T(K)$\sim$6.3; these loops would come determined by lower electron densities (log N$_e[cm^{-3}] \sim$9.5–10.5) as those measured in stars like α Cen, Procyon, ϵ Eri, Capella or AB Dor (Schmitt et al., 1996; Mewe et al., 1995; Drake et al., 1997; Laming & Drake, 1999; Laming, 1998; Brickhouse, 1996; Canizares et al., 2000; Güdel et al., 2001). The second kind of loops would be dominant in active binary systems, showing maximum temperature around log T(K)$\sim$6.9, and higher electron densities (log N$_e[cm^{-3}] \gtrsim$12.0). A third group of loops could be also present in the most active stars, peaking at some point with log T(K)$\gtrsim$7.3,

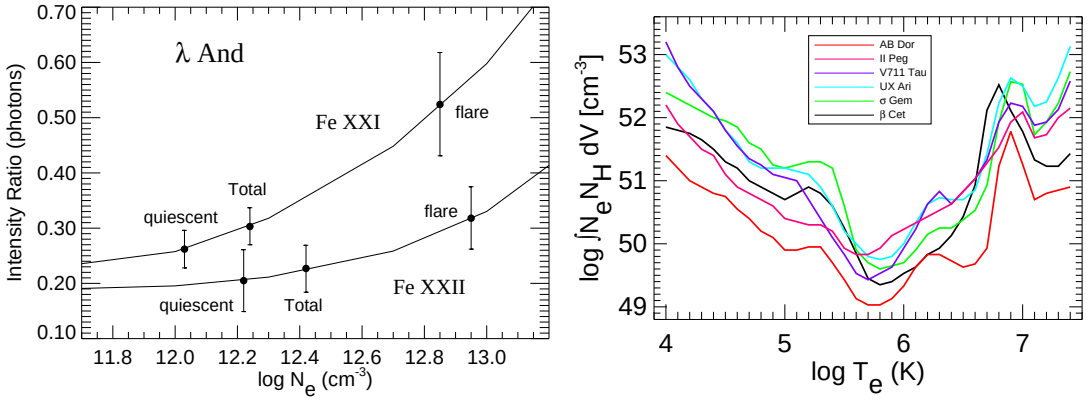

Figure 8. *Left*: Electron density derived from line ratio diagnostics from two different ionization stages of Fe. The line ratios shown are Fe XXI 102.22/128.73 and Fe XXII 114.41/117.17 for the quiescent and flare stages and the summed spectrum. The observed line ratios are plotted on the theoretical curves with 1-σ error bars representing the combined observational errors. *Right*: Comparison of the EMD obtained for 4 active binary systems (II Peg, V711 Tau, UX Ari, σ Gem), the young fast rotator AB Dor, and the evolved and apparently slow rotator β Cet.

although with the present data it is not possible to get better information for the material at these temperatures. This third group of loops would be involved in the large flares observed in the active binary systems, explaining why all the EMD is affected in this range in almost the same way. The persistency found in the presence of the bump at log T(K)$\sim$6.9 could be pointing to some kind of stability limit related to the formation of these loops.

Two recent works by Peres et al. (2000) and Reale, Peres, & Orlando (2001) analyzing the EMD of the Sun as a star show the presence of a bump during flares peaking around log T(K)$\sim$7.0. Although transient, this bump is reminiscent to those found in the stars of this sample, although with lower magnitude. This observation points towards solar-like flares as possible explanation to the bump observed in these stars, although that would bring strong energetic implications necessary to explain such stable bump in these stars by continous flaring. These flares would not be easily identified in the EUVE light curves due to their duration and magnitude.

5. Conclusions

Following conclusions can be obtained from the analysis of these data:

- 25 out of 28 stars in the sample show a narrow enhancement or "bump", peaking at log T(K)$\sim$6.8–7.0.
- This "bump" is present for single stars and binary systems.
- Possible 2^{nd} "bump" at log T(K)$\sim$6.3.

- Electron densities of log N_e(cm^{-3})$\sim$12–13.5 are measured at log T(K)$\sim$7.0, implying an emitting volume of 2–5$\times10^{26}$ cm^3.
- Presence of hotter (log T[K]$\gtrsim$7.0) material is detected in the most active stars.
- EMD may be characterized by contributions from:
  - solar-like loops (log T[K]$\sim$6.3), log N_e $\sim$9–10
  - expanding loops (log T[K]$\sim$6.9), log N_e $\gtrsim$12
  - hotter (log T[K]$\gtrsim$7.3) loops? These could be involved in the large flares observed in some of these systems.

Acknowledgments. This work has been made in collaboration with Dr. A. K. Dupree and Dr. N. S. Brickhouse, from the Harvard-Smithsonian Center for Astrophysics. This research is supported in part by NASA grant NAG5-7224 and the Predoctoral Program of the Smithsonian Astrophysical Observatory, and by the Real Colegio Complutense at Harvard. This research has made use of the SIMBAD database, operated at CDS, Strasbourg, France. This research has made use of data obtained through the High Energy Astrophysics Science Archive Research Center Online Service, provided by the NASA/Goddard Space Flight Center.

References

Allen, C. W. 1973, Astrophysical quantities (London: University of London, Athlone Press, —c1973, 3rd ed.)

Anders, E. & Grevesse, N. 1989, Geochim. Cosmochim. Acta, 53, 197

Brickhouse, N. S. 1996, in IAU Colloq. 152: Astrophysics in the Extreme Ultraviolet, (Dordrecht: Kluwer Academic Publ.), ed. by S. Bowyer and R. F. Malina, p. 105

Brickhouse, N. S. & Dupree, A. K. 1998, ApJ, 502, 918

Brickhouse, N. S., Raymond, J. C., & Smith, B. W. 1995, ApJS, 97, 551

Canizares, C. R., et al. 2000, ApJ, 539, L41

Drake, J. J., Laming, J. M., & Widing, K. G. 1997, ApJ, 478, 403

Dupree, A. K., Brickhouse, N. S., Doschek, G. A., Green, J. C., & Raymond, J. C. 1993, ApJ, 418, L41

Griffin, R. F. 1998, The Observatory, 118, 273

Griffiths, N. W. 1999, ApJ, 518, 873

Griffiths, N. W. & Jordan, C. 1998, ApJ, 497, 883

Güdel, M., Audard, M., Briggs, K., Haberl, F., Magee, H., Maggio, A., Mewe, R., Pallavicini, R., & Pye, J. 2001, A&A, 365, L336

Hussain, G. A. 2001, This issue

Jordan, C. 1996, in IAU Colloq. 152: Astrophysics in the Extreme Ultraviolet, (Dordrecht: Kluwer Academic Publ.), ed. by S. Bowyer and R. F. Malina, p. 81

Laming, J. M. 1998, in ASP Conf. Ser. 154: Cool Stars, Stellar Systems, and the Sun, Vol. 10, ed. by R. A. Donahue and J. A. Bookbinde, p. 447

Laming, J. M. & Drake, J. J. 1999, ApJ, 516, 324

Mewe, R., Kaastra, J. S., Schrijver, C. J., van den Oord, G. H. J., & Alkemade, F. J. M. 1995, A&A, 296, 477

Peres, G., Orlando, S., Reale, F., Rosner, R., & Hudson, H. 2000, ApJ, 528, 537

Raymond, J. C. 1988, in NATO ASIC Proc. 249: Hot Thin Plasmas in Astrophysics, ed. R. Pallavicini, 3

Reale, F., Peres, G., & Orlando, S. 2001, ApJ, 557, 906

Sanz-Forcada, J. 2001, PhD thesis, University Complutense of Madrid

Sanz-Forcada, J., Brickhouse, N. S., & Dupree, A. K. 2001a, ApJ, 554, 1079

—. 2001b, ApJ, submitted

—. 2001c, ApJS, submitted

Schmitt, J. H. M. M. 1998, in ASP Conf. Ser. 154: Cool Stars, Stellar Systems, and the Sun, Vol. 10, ed. by R. A. Donahue and J. A. Bookbinde, p. 463

Schmitt, J. H. M. M., Drake, J. J., Stern, R. A., & Haisch, B. M. 1996, ApJ, 457, 882

Schrijver, C. J., Lemen, J. R., & Mewe, R. 1989, ApJ, 341, 484